Dear Author,

Here are the proofs of your article.

- You can submit your corrections **online**, via **e-mail** or by **fax**.
- For **online** submission please insert your corrections in the online correction form. Always indicate the line number to which the correction refers.
- You can also insert your corrections in the proof PDF and **email** the annotated PDF.
- For fax submission, please ensure that your corrections are clearly legible. Use a fine black pen and write the correction in the margin, not too close to the edge of the page.
- Remember to note the **journal title**, **article number**, and **your name** when sending your response via e-mail or fax.
- **Check** the metadata sheet to make sure that the header information, especially author names and the corresponding affiliations are correctly shown.
- **Check** the questions that may have arisen during copy editing and insert your answers/ corrections.
- **Check** that the text is complete and that all figures, tables and their legends are included. Also check the accuracy of special characters, equations, and electronic supplementary material if applicable. If necessary refer to the *Edited manuscript*.
- The publication of inaccurate data such as dosages and units can have serious consequences. Please take particular care that all such details are correct.
- Please **do not** make changes that involve only matters of style. We have generally introduced forms that follow the journal's style.
  Substantial changes in content, e.g., new results, corrected values, title and authorship are not allowed without the approval of the responsible editor. In such a case, please contact the Editorial Office and return his/her consent together with the proof.
- If we do not receive your corrections **within 48 hours**, we will send you a reminder.
- Your article will be published **Online First** approximately one week after receipt of your corrected proofs. This is the **official first publication** citable with the DOI. **Further changes are, therefore, not possible.**
- The **printed version** will follow in a forthcoming issue.

Please note

After online publication, subscribers (personal/institutional) to this journal will have access to the complete article via the DOI using the URL: http://dx.doi.org/[DOI].
If you would like to know when your article has been published online, take advantage of our free alert service. For registration and further information go to: http://www.link.springer.com.

Due to the electronic nature of the procedure, the manuscript and the original figures will only be returned to you on special request. When you return your corrections, please inform us if you would like to have these documents returned.

Metadata of the article that will be visualized in OnlineFirst

ArticleTitle	Diffusion Multiples as a Tool to Efficiently Explore the Composition Space of High Entropy Alloys	
Article Sub-Title		
Article CopyRight	ASM International (This will be the copyright line in the final PDF)	
Journal Name	Journal of Phase Equilibria and Diffusion	
Corresponding Author	Family Name	**Jacques**
	Particle	
	Given Name	**P. J.**
	Suffix	
	Division	Institute of Mechanics, Materials and Civil Engineering, IMAP
	Organization	UCLouvain
	Address	Place Sainte Barbe 2, 1348, Louvain-la-Neuve, Belgium
	Phone	
	Fax	
	Email	antoine.hilhorst@uclouvain.be
	URL	
	ORCID	
Author	Family Name	**Hilhorst**
	Particle	
	Given Name	**A.**
	Suffix	
	Division	Institute of Mechanics, Materials and Civil Engineering, IMAP
	Organization	UCLouvain
	Address	Place Sainte Barbe 2, 1348, Louvain-la-Neuve, Belgium
	Phone	
	Fax	
	Email	
	URL	
	ORCID	
Schedule	Received	31 March 2021
	Revised	23 May 2021
	Accepted	31 May 2021

Abstract

The concept of high entropy alloys (HEAs) has already provided specific alloys presenting improved structural and functional properties. However, the discovery and development of new HEAs still represent a big challenge due to their chemical complexity. Diffusion multiples can be used as an experimental approach to screen large composition ranges. The method consists in heat-treating intimately bonded metallic blocks to activate diffusion, thus creating gradients of compositions. Local chemical and physical properties can be directly probed using advanced characterization techniques. The measured characteristics and properties can be further analysed to estimate diffusion properties or mechanical properties. In the present study, four different diffusion multiples related to the Cantor alloy system, Cr-Fe-Mn-Co-Ni, were investigated. Resulting microstructures were investigated after several heat treatments to assess the claimed entropy-based stabilization of a single phase. Crystallographic characterization by EBSD coupled to EDX

	mapping were compared to Calphad predictions. Local nano-indentation mapping was carried out and compared to the prediction of the yield strength model proposed by Walbrühl et al. (Mater Sci Eng A 700: 301–311, 2017, https://doi.org/10.1016/j.msea.2017.06.001). This article is part of a special topical focus in the Journal of Phase Equilibria and Diffusion on the Thermodynamics and Kinetics of High-Entropy Alloys. This issue was organized by Dr. Michael Gao, National Energy Technology Laboratory; Dr. Ursula Kattner, NIST; Prof. Raymundo Arroyave, Texas A&M University; and the late Dr. John Morral, The Ohio State University.
Keywords (separated by '-')	CALPHAD - diffusion multiples - high entropy alloys
Footnote Information	This article is part of a special topical focus in the Journal of Phase Equilibria and Diffusion on the Thermodynamics and Kinetics of High-Entropy Alloys. This issue was organized by Dr. Michael Gao, National Energy Technology Laboratory; Dr. Ursula Kattner, NIST; Prof. Raymundo Arroyave, Texas A&M University; and the late Dr. John Morral, The Ohio State University **Supplementary Information** The online version contains supplementary material available at https://doi.org/10.1007/s11669-021-00902-z.

J. Phase Equilib. Diffus.
https://doi.org/10.1007/s11669-021-00902-z

Diffusion Multiples as a Tool to Efficiently Explore the Composition Space of High Entropy Alloys

A. Hilhorst[1] · P. J. Jacques[1]

Submitted: 31 March 2021 / in revised form: 23 May 2021 / Accepted: 31 May 2021

Abstract The concept of high entropy alloys (HEAs) has already provided specific alloys presenting improved structural and functional properties. However, the discovery and development of new HEAs still represent a big challenge due to their chemical complexity. Diffusion multiples can be used as an experimental approach to screen large composition ranges. The method consists in heat-treating intimately bonded metallic blocks to activate diffusion, thus creating gradients of compositions. Local chemical and physical properties can be directly probed using advanced characterization techniques. The measured characteristics and properties can be further analysed to estimate diffusion properties or mechanical properties. In the present study, four different diffusion multiples related to the Cantor alloy system, Cr-Fe-Mn-Co-Ni, were investigated. Resulting microstructures were investigated after several heat treatments to assess the claimed entropy-based stabilization of a single phase. Crystallographic characterization by EBSD coupled to EDX mapping were compared to Calphad predictions. Local nano-indentation mapping was carried out and compared to the prediction of the yield strength model proposed by Walbrühl et al. (Mater Sci Eng A 700: 301–311, 2017, https://doi.org/10.1016/j.msea.2017.06.001). This article is part of a special topical focus in the Journal of Phase Equilibria and Diffusion on the Thermodynamics and Kinetics of High-Entropy Alloys. This issue was organized by Dr. Michael Gao, National Energy Technology Laboratory; Dr. Ursula Kattner, NIST; Prof. Raymundo Arroyave, Texas A&M University; and the late Dr. John Morral, The Ohio State University.

Keywords CALPHAD · diffusion multiples · high entropy alloys

1 Introduction

High entropy alloys (HEAs) have gathered a lot of attention in recent years. Such alloys explore composition ranges never investigated before while promising exceptional levels or combinations of properties.[2–7] In contrast to conventional alloys, HEAs are fundamentally made of multi-principal elements, typically 3 to 5 (or even more), at large concentrations.[8,9] One of the most studied HEA system is the Co-Cr-Fe-Mn-Ni system, known as the "Cantor alloy",[10] presenting a stable face centred cubic (FCC) solid solution at room temperature[11] in the case of the equimolar alloy. It exhibits excellent deformability thanks to the activation of mechanical twinning,[12] good corrosion resistance,[13] and exceptional fracture toughness.[14,15] Due to the inherent chemical complexity of HEAs, conventional tools for thermodynamic description of stability are not always adapted or accurate enough. The latest CALPHAD (Calculation of Phase Diagrams) databases are not large enough, even in the case of well-studied HEAs such as the Co-Cr-Fe-Mn-Ni system[16,17] to always reach the adequate level of predictability.

This article is part of a special topical focus in the Journal of Phase Equilibria and Diffusion on the Thermodynamics and Kinetics of High-Entropy Alloys. This issue was organized by Dr. Michael Gao, National Energy Technology Laboratory; Dr. Ursula Kattner, NIST; Prof. Raymundo Arroyave, Texas A&M University; and the late Dr. John Morral, The Ohio State University

✉ P. J. Jacques
antoine.hilhorst@uclouvain.be

[1] Institute of Mechanics, Materials and Civil Engineering, IMAP, UCLouvain, Place Sainte Barbe 2, 1348 Louvain-la-Neuve, Belgium

Journal : Large 11669 | Dispatch : 24-6-2021 | Pages : 12
Article No. : 902 | ☐ LE | ☐ TYPESET
MS Code : JPED-21-03-2509 | ☑ CP | ☑ DISK

Experimentally speaking, several methods exist to explore large ranges of composition, some of them already used in the case of HEAs.[18–21] One of such high-throughput methods is the use of diffusion multiples.[22] This method consists in heat-treating assemblies of pieces of pure metals or alloys to activate diffusion and consequently create gradients of compositions. Diffusion multiples have been used extensively to gather data in the case of ternary systems, for example.[23,24]

Kaufman et al.[25,26] reported a detailed analysis of a diffusion multiple composed of pure Cr, Fe-50Mn, and Co-50Ni (in at.%) heat treated for 24 h at 1000 °C. While they focused on the solid solution strengthening operating in HEAs, hardly anything has been reported about the complete analysis of the Cr-Mn-Fe-Co-Ni system.

A new methodology of assessment of multinary diffusion multiples is proposed in the present study. To achieve this objective, four diffusion multiples have been manufactured from different pieces of unary or binary alloys of the Cantor constitutive elements. Indeed, obtaining a quinary junction between five elementary blocks would be very difficult. Furthermore, it would also impose a specific configuration of the diffusion paths. It was therefore decided to assess the quinary system by observing several diffusion multiples made of three-blocks obtained after a two-step joining and diffusion process. Using this method, at least one block must contain more than one element. One such diffusion multiple is arguably not enough to explore a compositionally complex system containing five elements. Indeed, it is worth emphasizing that the number of diffusion paths increases with the number of constitutive elements. Consequently, while it is expected to find an area presenting the equiatomic CrMnFeCoNi composition for any diffusion multiple, the surrounding compositions would have to be investigated from different starting phases. Therefore, analysing the influence of the geometrical repartition of the five elements requires the investigation of several diffusion multiples for the same system. Furthermore, using pieces of two binary systems and one unary system allows the concomitant analysis of one quaternary junction and two ternary junctions. The effect of increasing amounts of alloying elements can be studied by following the ternary or quaternary junction towards the centre of the diffusion multiple. Finally, repeating ternary junctions can be useful to deduce (inter-)diffusion coefficients.[27–29]

Beside thermodynamic stability, the adjustment of the constitutive phases also plays an important role on the resulting mechanical behaviour. BCC phase is generally a stronger but less ductile phase while FCC phase is generally softer but more ductile. Moreover, transformation-induced plasticity (TRIP) and twinning-induced plasticity (TWIP)[30] are two mechanisms that are of great interest to design alloys with improved balance of strength and ductility,[31] sometimes in relationship with HCP phase transformation. Understanding the role of each element of a complex system on the activated plasticity mechanisms is thus of great importance for alloy design.

Finally, thermodynamic equilibrium can be investigated at different temperatures thanks to this methodology. Indeed, once it is processed, it is easy to slice the diffusion multiple into several samples that can be individually heat treated. In this study, two heat treatments were applied to each diffusion multiples: a high temperature treatment at 1000 °C for 24 h and a low temperature treatment at 425 °C for 4 days. The high temperature treatment mostly corresponds to the homogenisation temperature applied to HEAs in most studies. The low temperature treatment was chosen to assess the Cantor system in conditions scarcely reported in the literature. Moreover, there are concerns about single phase stability in HEAs during long term annealing at temperatures below 500 °C.[32–34] For instance, CoCrFeMnNi decomposes to sigma phase,[35,36] which is very detrimental to its mechanical properties.

2 Methods

Four different diffusion multiples comprising 3 parts were processed. The multiples were first bonded in a two-step process by first bonding a block “A” with a block “B”, then repeating the process to bond the formed couple “A-B” to a third block “C”. The diffusion multiples will be designated by “A-B-C”, with the composition mentioned (in atomic percentage). The bonding heat treatment was carried out using either a clamp in a tubular furnace with a constant argon flow, or a high temperature uniaxial press working under vacuum. Details of the heat treatment process for each diffusion multiple are given in Table 1 and Fig. 1. The constitutive alloys were all prepared by arc melting of pure elements (> 99.9% purity). Manganese chips were deoxidised prior to casting using 50% HCl solution. After casting, the ingots were machined to the appropriate size and the bonding surface was mechanically polished down to 1 µm to ensure a good bonding. Heat treatments of 1000 °C for 24 h and of 425 °C for 4 days were then carried out on samples cut from each diffusion multiples and sealed in argon-filled quartz capsules. The samples were water quenched to avoid phase transformation during cooling. However, this does not prevent displacive transformation from occurring.

It is worth noting that manganese oxides are present in all diffusion multiples containing the alloy FeMn as fully deoxidising the manganese before arc melting is very tricky. Two multiples FeMn-CoNi-Cr were processed differing by the presence of residual carbon in one of them. In

Journal : Large 11669 Dispatch : 24-6-2021 Pages : 12
Article No. : 902 LE TYPESET
MS Code : JPED-21-03-2509 CP DISK

Table 1 Composition and bonding heat treatment of the studied diffusion multiples

Sample name	Heat treatment	
	A to B	A-B to C
FeMn-CoNi-Cr	Uniaxial press under vacuum	Uniaxial press under vacuum
	1000N applied force	800N applied force
	1000 °C for 1 h	900 °C for 1 h
	25 °C/min heating rate	25 °C/min heating rate
	Air quench	Air quench
FeMn-CoNi-Cr168C	Tubular furnace in Ar flow	Tubular furnace in Ar flow
	Clamp with 4 screws torqued at 8 Nm	Clamp with 4 screws torqued at 8 Nm
	1000 °C 1 h	1000 °C 1 h
	50 °C/min heating rate	50 °C/min heating rate
	Air quench	Air quench
Co-CrNi-FeMn	Tubular furnace in Ar flow	Tubular furnace in Ar flow
	Clamp with 4 screws torqued at 8 Nm	Clamp with 4 screws torqued at 8 Nm
	1000 °C 1 h	1000 °C 1 h
	50 °C/min heating rate	50 °C/min heating rate
	Air quench	Air quench
Co30Cr-Ni-FeMn	Uniaxial press under vacuum	Uniaxial press under vacuum
	900N applied force	1000N applied force
	1000 °C for 1 h	1000 °C for 1 h
	25 °C/min heating rate	25 °C/min heating rate
	Air quench	Air quench
CoFe-MnNi-Cr	Uniaxial press under vacuum	Uniaxial press under vacuum
	800 N applied force	800 N applied force
	900 °C for 1 h	800 °C for 1 h
	25 °C/min heating rate	25 °C/min heating rate
	Air quench	Air quench

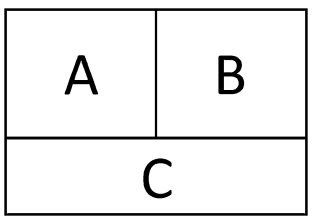

Fig. 1 Schematic representation of a diffusion multiple sections. The bonding order is A to B, then A-B to C

that case, the used Cr chips contained 168 ppm of C. This sample is referred as FeMn-CoNi-Cr168C.

In the case of blocks made of binary alloys, prior check of the phase diagrams is worth being carried out to avoid potential experimental difficulties. For example, the diffusion multiple Co-CrNi-FeMn contains the binary Cr50Ni. This alloy is not a solid solution but a dual phase alloy at equilibrium at 1000 °C with 22% of a Cr-rich phase and 78% of a Ni-rich phase.[37] For Co30Cr-Ni-FeMn, Co-30Cr was used instead of an equiatomic CoCr alloy because this last equiatomic alloy would have contained a large proportion of σ phase which is very brittle, whereas the Co-30Cr alloy is single phase (α-Co).[38] Additionally, the alloy MnNi in the diffusion multiple CoFe-MnNi-Cr has the lowest melting temperature of the order of 1050 °C.[39] To avoid a large deformation during the hot-pressing stage, this diffusion multiple was bonded at a lower temperature. Nevertheless, processing CoFe-MnNi-Cr at this temperature caused the interface between the block MnNi and CoFe to be curved, as shown hereunder.

The proposed choice of diffusion multiples leads to the creation of 4 unique quaternaries and 5 unique ternaries. The ternary CoCrNi system, another alloy of large interest[40–42] for its mechanical properties, is repeated three times within the multiples. The system FeMnNi is repeated twice.

The heat-treated samples were characterized by scanning electron microscopy (SEM) operated at 15 kV, with energy dispersive x-ray analysis (EDX) for chemical mapping and electron backscatter diffraction (EBSD) for phase and crystallographic mapping. Sample preparation consisted in polishing mounted samples down to 1 µm and then with oxide polishing suspension (OP-S). Regions of

Journal : Large 11669 Dispatch : 24-6-2021 Pages : 12
Article No. : 902 LE TYPESET
MS Code : JPED-21-03-2509 CP DISK

interest were further characterised by EBSD for phase identification. Mapping of local hardness was carried out using nano-indentation performed using an Agilent G200 equipment with a Berkovitch tip and a set displacement depth of 100 nm. Analysis of nano-indentation results were carried out in part using the TriDiMap Matlab Toolbox.[43]

Focused ion beam (FIB) machined specific zones of the carbon-added multiple were characterized by transmission electron microscopy (TEM). TEM analyses were performed on a Tecnai F20 G2 TEM operated at 200 kV.

Thermo-Calc[44] version 2021a with TCHEA2.1 and TCFE10 databases was used to predict phase stability and hardness[1] of the investigated diffusion multiples. For phase predictions, the fractions of FCC, BCC, HCP (if relevant) and ordered phases were computed and then displayed considering a colour coding based on the three fundamental colours, i.e., red, green, and blue (RGB). Red colour was attributed to the BCC phase, blue to FCC and green to intermetallic phases. In the few cases where HCP phase was present, it was represented as yellow. For the yield strength prediction, the model assumes only solid solution strengthening. Grain boundary and precipitation strengthening are not considered. Yield strength is evaluated at 300 K for an equilibrium considered at 1273 K.

3 Results

Representative SEM and EDX mappings of the diffusion multiples FeMn-CoNi-Cr, Co-CrNi-FeMn, Co30Cr-Ni-FeMn, and MnNi-CoFe-Cr are given in Fig. 2 for the FeMn-CoNi-Cr multiple after 1000 °C for 24 h. The SEM and EDX mappings of each diffusion multiple and for both heat treatments are provided in the supplementary materials. Good bonding between the different blocks can be observed for the different diffusion multiples. However, large porosities can be sometimes observed, due to the well-known Kirkendall effect,[46,47] even though it is less pronounced at 425 °C.

Some phases are significantly more etched than others due to different reactivity with the OP-S solution. In particular, the FeMn pieces were rapidly corroded during the OP-S polishing. This affects the indexing rate of EBSD measurements but was up to now unavoidable.

3.1 FeMn-CoNi-Cr Multiple

At 1000 °C, three different phases can be observed in FeMn-CoNi-Cr (excluding the Mn oxides). Initial Cr, CoNi and FeMn alloys are BCC, FCC, and FCC, respectively. Sigma phase is present at the boundary between Cr and CoNi alloys or between Cr and FeMn alloys, as shown in Fig. 3. Sigma phase is expected to appear at equilibrium at 1000 °C for Cr rich alloy both in ternary CrFeMn and CrCoNi alloys.[48,49] Interestingly, FCC grains can be observed between the sigma phase and the Cr-rich BCC area at the junction between CoNi and Cr pieces, as shown in the magnified inset of Fig. 3.

The microstructure at the ternary junction of FeMn-CoNi-Cr and FeMn-CoNi-Cr168C multiples varies greatly. Special care was used to characterize the phases formed at the triple junction between FeMn, CoNi, and Cr of the

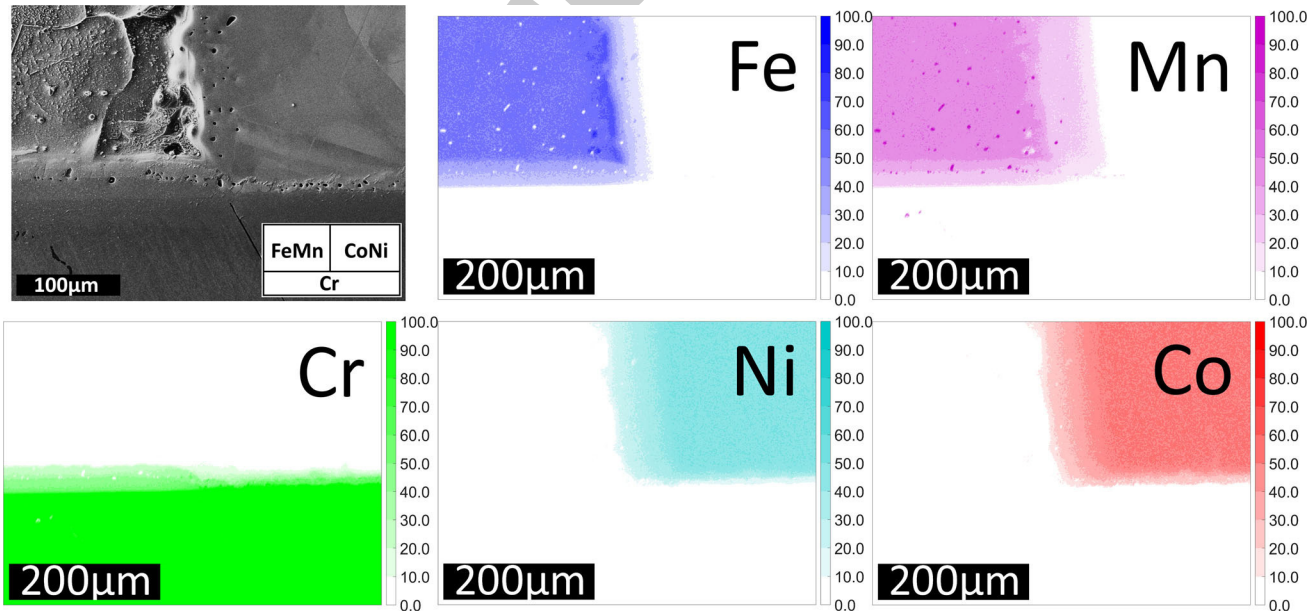

Fig. 2 SEM micrograph and EDX composition maps of the constitutive elements of diffusion multiple FeMn-CoNi-Cr at the ternary junction after a heat treatment of 1000 °C for 24 h

Journal : Large 11669 Dispatch : 24-6-2021 Pages : 12
Article No. : 902 LE TYPESET
MS Code : JPED-21-03-2509 CP DISK

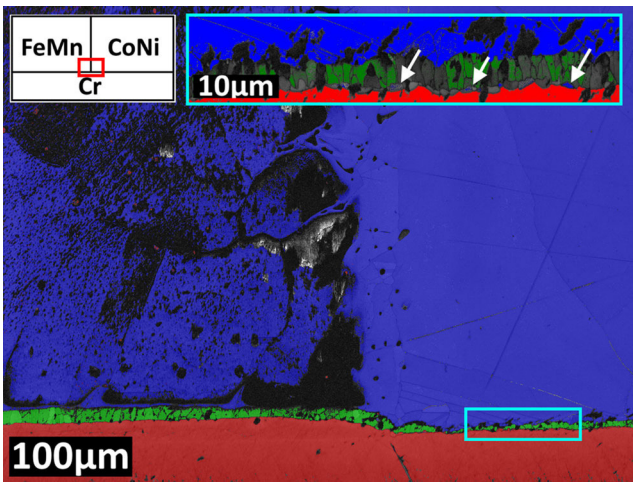

Fig. 3 EBSD phase and band contrast map of the FeMn-CoNi-Cr multiple at the ternary junction after 24 h at 1000 °C. FCC phase is highlighted in blue, BCC phase in red, sigma phase in green

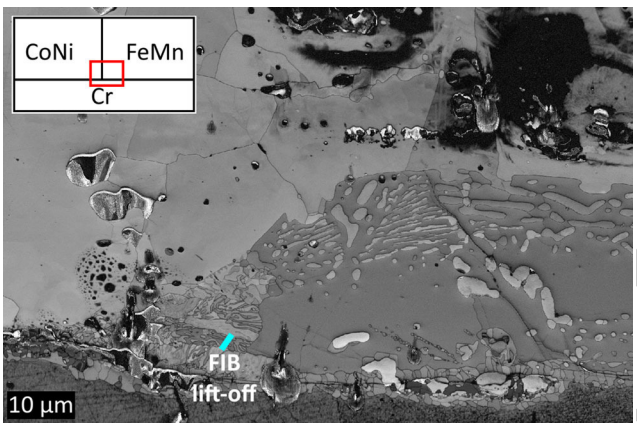

Fig. 4 EBSD band contrast map of the triple junction of sample FeMn-CoNi-Cr168C after 24 h at 1000 °C. The location where the TEM thin foil was FIBed is also indicated

FeMn-CoNi-Cr168C diffusion multiple. EBSD maps and TEM micrographs with the corresponding diffraction diagrams of regions of interest are given in Fig. 4 and 5, respectively. In this high mixing region, microstructure decomposes into two phases with elongated grains of around 1 µm width in the case of the FeMn-CoNi-Cr168C. Thanks to the diffraction patterns, the Cr and C rich phase can be associated with a $M_{23}C_6$-type carbide and the second phase with a disordered FCC phase. The composition of the FCC phase measured by TEM-EDX is Cr21.2Mn20.8Fe36.3Co11.1Ni10.6 with a lattice parameter of 0.357 nm.

The carbon addition also impacted sigma phase formation. Indeed, sigma phase is not observed at the boundary between CoNi and Cr blocks. However, this sigma phase is more prominent between FeMn and Cr blocks in the FeMn-CoNi-Cr168C multiple than in the FeMn-CoNi-Cr multiple. The layer of sigma phase is about 10 µm thick in FeMn-CoNi-Cr and close to 30 µm in FeMn-CoNi-Cr168C.

For the heat treatment at 425 °C for 4 days, the diffusion length is significantly smaller across all interfaces compared to the high temperature heat treatment. In consequence, regions of interest with high mixing between 4 or 5 elements are limited. The microstructures observed by SEM are like an untreated sample.

3.2 Co-CrNi-FeMn Multiple

Figure 6 shows that mostly FCC and HCP phases are present in the Co-CrNi-FeMn multiple. There is a small amount of BCC phase in the CrNi block as equilibrium at this temperature consists of a small amount of Cr-rich BCC phase in an FCC matrix. HCP can also be observed within the dominant FCC phase in a small region where the three blocks meet, as seen in the magnified inset of Fig. 6.

The region of interest with high mixing where both FCC and HCP phases coexist has been further analysed with nano-indentation. Figure 7 shows the SEM micrograph after the indentation mapping (a), the corresponding measured hardnesses (b,c), and the composition maps measured by EDX associated to the indentation mapping (d). From the corresponding compositions, the yield strength has been computed using Thermo-Calc property model, shown in Fig. 7(c).

3.3 Co30Cr-Ni-FeMn Multiple

Only FCC and HCP phases are present in the Co30Cr-Ni-FeMn multiple, as shown in Fig. 8. FCC grains can be observed in the HCP phase of CoCr close to the boundary with FeMn. This would indicate that FCC and HCP in this composition range are close in energy.

3.4 CoFe-MnNi-Cr Multiple

Finally, in the case of the CoFe-MnNi-Cr multiple, only BCC and FCC phases are observed, as shown in Fig. 9. During the second bonding step, due to the large softening of the MnNi block, the boundary between the blocks is not as clear as for the other diffusion multiples. We can also observe that a transformation occurred during the cooling of a region where it is mostly Mn and Ni where needle-shaped grains appeared.

Journal : Large 11669 Dispatch : 24-6-2021 Pages : 12
Article No. : 902 LE TYPESET
MS Code : JPED-21-03-2509 CP DISK

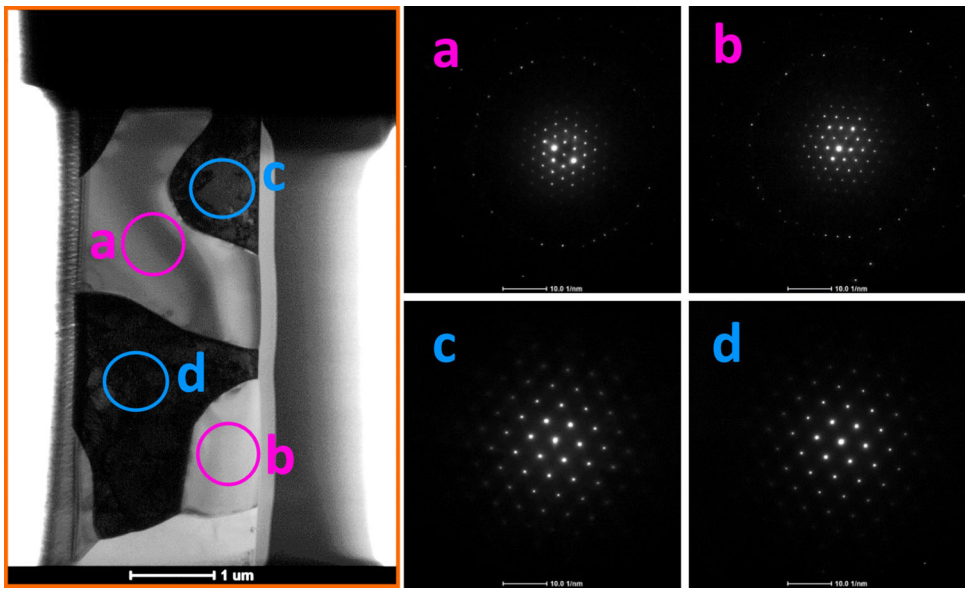

Fig. 5 TEM micrograph associated to the FIB slice of sample FeMn-CoNi-Cr168C after 24 h at 1000 °C. Selected area electron diffraction patterns are given for 4 regions a through d. Patterns a and b correspond to M23C6 and pattern c and d correspond to FCC phase with a = 0.357 nm

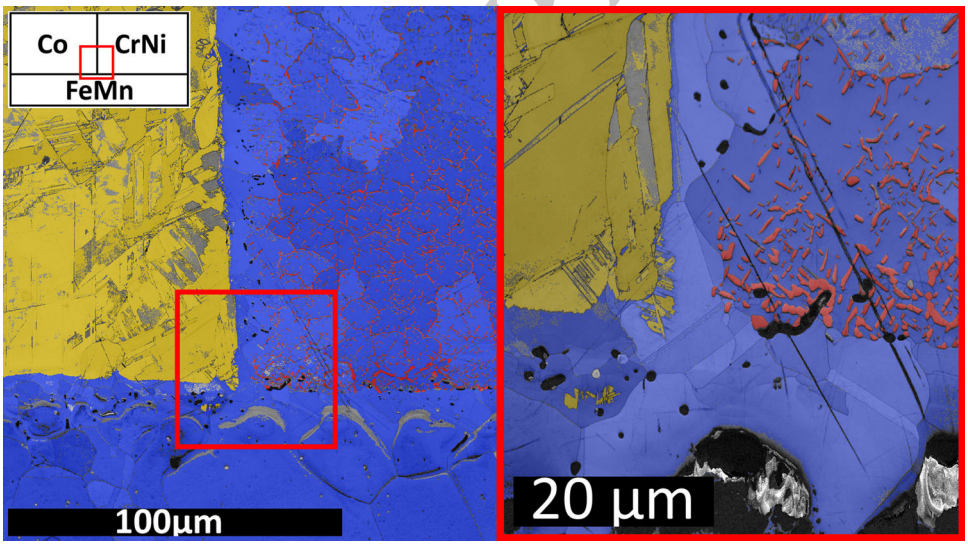

Fig. 6 EBSD phase and band contrast map of the Co-CrNi-FeMn multiple at the ternary junction after 24 h at 1000 °C. FCC phase is highlighted in blue, BCC phase in red, HCP phase in yellow

4 Discussion

Diffusion multiples offer a large range of results than can be interpreted to show different facets of an alloy system. Here, we discuss the impact of the results on phase prediction, inter-diffusion, and mechanical properties.

4.1 Phase Prediction

Diffusion multiples were mostly used, up to now, to study ternary systems to feed modelling databases. It is worth noting that even with the currently large interest for HEAs, the latest Thermo-Calc databases are not fully assessed yet.[16,50] Indeed, even in the case of the most studied Cantor system, six from the ten constitutive ternaries are not fully assessed in TCHEA2.1 database, down to five in the latest version. Furthermore, thermodynamic data of Mn-based systems are also hard to obtain. TCFE10 database, the steel and iron alloys database, is also used in this study. This database can be suitable for Cantor-based system as the recommended composition limits on its constitutive elements are 30 wt.% max for Cr and Mn and 20 wt.% max for Co and Ni. Nevertheless, several ternaries of CrMnFeCoNi are not fully assessed in this database neither. As such, diffusion multiples are an important and effective tool to improve the current state of modelling and predictions based on the CALPHAD approach.

Other predictive tools are developed, but large enough sets of experimental data to validate or, in the case of neural network-based tools, to train the proposed models are also not easily accessible [51–53]. Published studies are mostly focused on a small subset of elements [8] and recent

Journal : Large 11669 | Dispatch : 24-6-2021 | Pages : 12
Article No. : 902 | LE | TYPESET
MS Code : JPED-21-03-2509 | CP | DISK

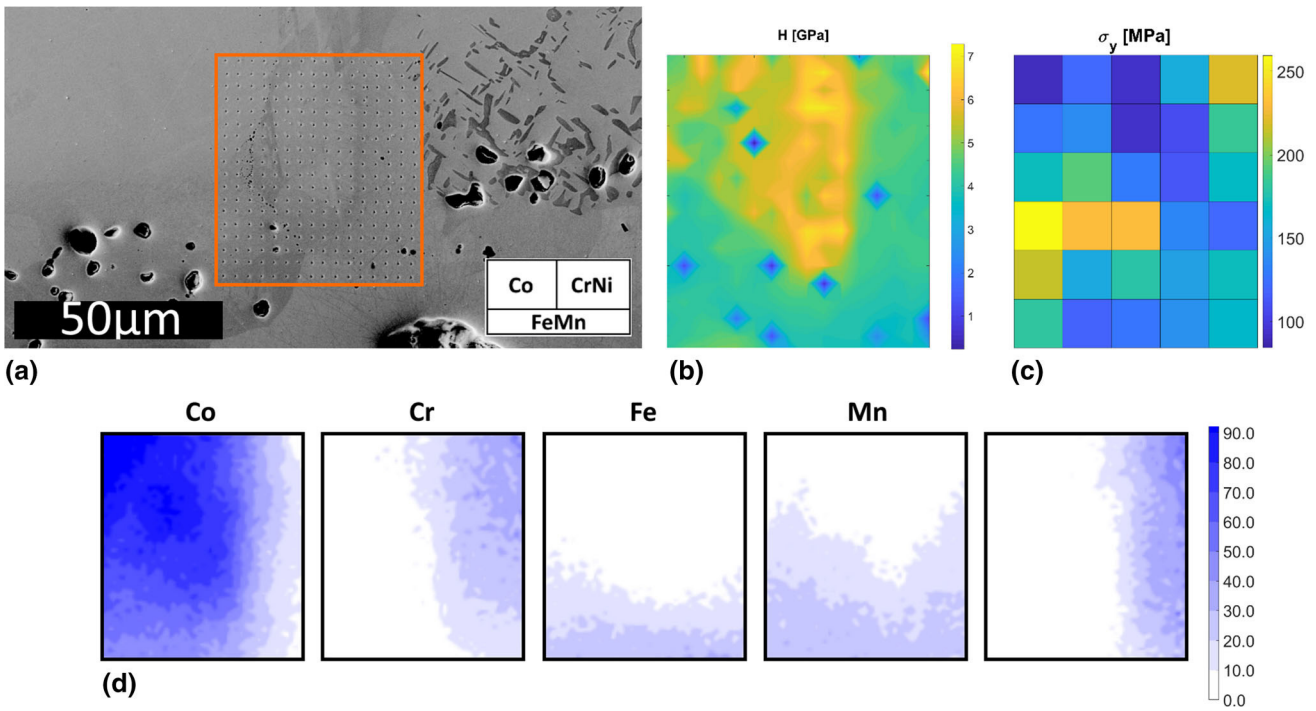

Fig. 7 (a) SEM micrograph of the diffusion multiple Co-CrNi-FeMn after nanoindentation mapping at the triple junction, (b) the associated hardness map obtained from nanoindentation measurements; (c) the predicted yield strength map obtained from Thermo-Calc property model calculator; and (d) the composition maps from EDX measurements for each constitutive element corresponding to the highlighted region

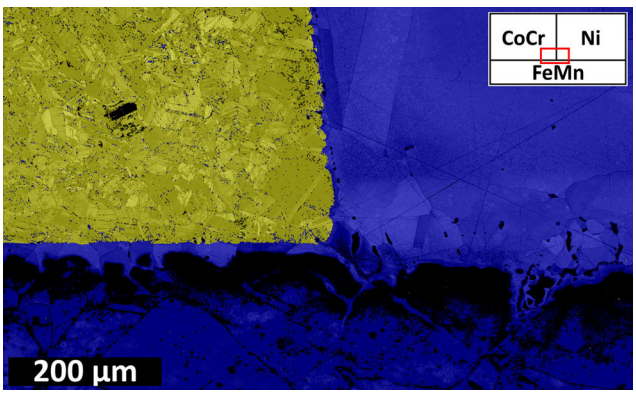

Fig. 8 EBSD phase and band contrast map of the Co30Cr-Ni-FeMn multiple at the ternary junction after 24 h at 1000 °C. FCC phase is highlighted in blue, HCP phase in yellow

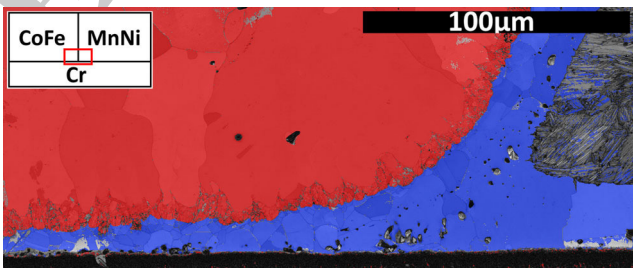

Fig. 9 EBSD phase and band contrast map of the CoFe-MnNi-Cr multiple at the ternary junction after 24 h at 1000 °C. FCC phase is highlighted in blue, BCC phase in red

developments focus on the optimization of known HEA systems rather than new combinations of elements. Furthermore, the microstructural state is often far from thermodynamic equilibrium [17,54].

The local phase identification carried out by EBSD for the four diffusion multiples (summarised in Table 1) can be compared to the predictions of the CALPHAD modelling, using the full ranges of compositions. Phase prediction in the case of diffusion for 1 day at 1000 °C is shown in Fig. 10, and in Fig. 11 for 4 days at 425 °C, for both the TCHEA2.1 and the TCFE10 databases. Surprisingly, the HCP phase is not predicted by Thermo-Calc for any of the different investigated composition ranges for both databases. Consequently, the predicted maps are built based on 3 phases, BCC, FCC and intermetallics (IM).

EBSD measurements showed that after the heat treatment conducted at 1000 °C, CoFe is BCC, Co30Cr and Co are HCP (Fig. 6, 8, and 9), whereas they are all predicted as FCC by Thermo-Calc. In the case of an equimolar CoFe alloy, the use of the TCHEA2.1 database predicts a phase change from BCC at low temperature to FCC at high temperature at 970 °C. In the case of the Co30Cr alloy and Co, there is a transition from HCP to FCC at 900 °C and 422 °C, respectively. The FCC phase tends to dominate

Journal : Large 11669 Dispatch : 24-6-2021 Pages : 12
Article No. : 902 LE TYPESET
MS Code : JPED-21-03-2509 CP DISK

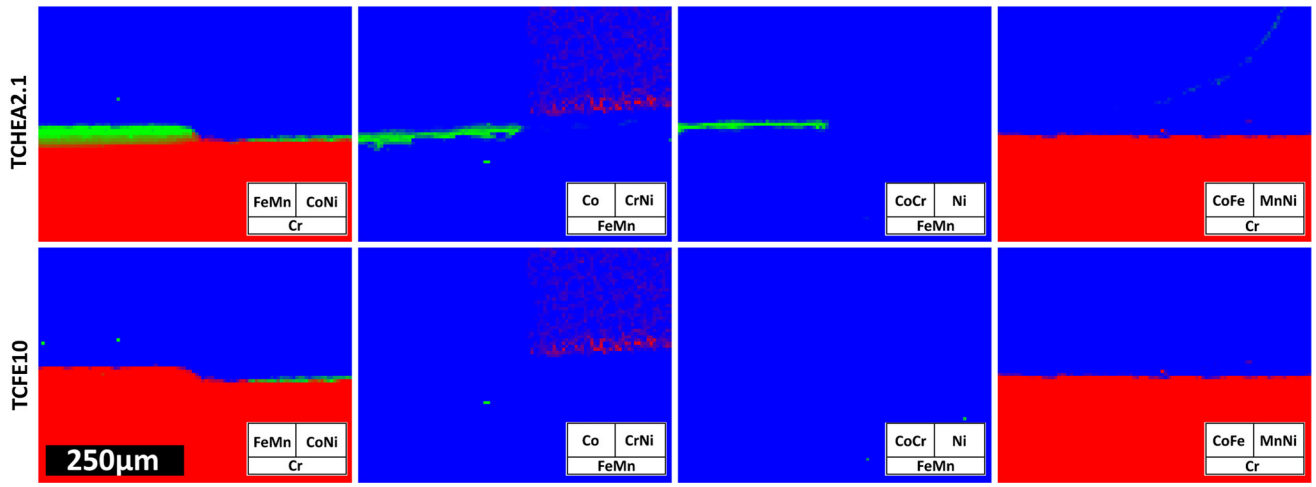

Fig. 10 Comparison of predictions from Thermo-Calc between the TCHEA2.1 and the TCFE10 databases for the four studied diffusion multiples after 1000 °C for 24h. Composition are measured by EDX. FCC phase is represented in blue, BCC phase in red, and intermetallics in green

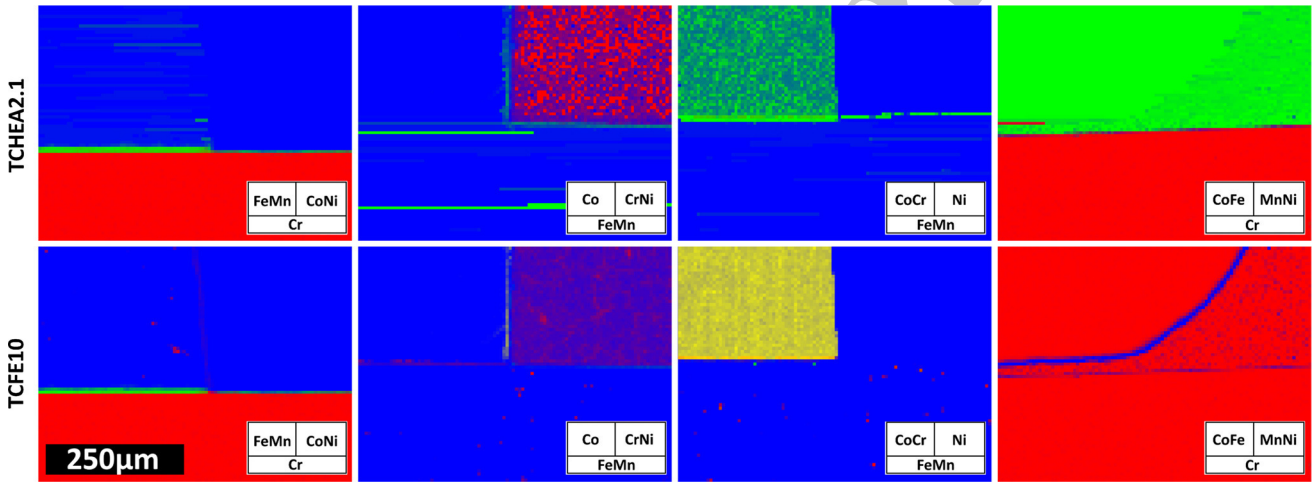

Fig. 11 Comparison of predictions from Thermo-Calc between the TCHEA2.1 and the TCFE10 databases for the four studied diffusion multiples after 425 °C for 4 days. Composition is measured by EDX. FCC phase is represented in blue, BCC phase in red, HCP phase in yellow, and intermetallics in green

other disordered phases using Thermo-Calc. By analysing the inverse pole figure maps and the microstructure morphology, martensitic transformation could have occurred during quenching for CoFe, Co30Cr, or Co which could explain the discrepancy between the EBSD measurements and the Thermo-Calc predictions.

For the prediction of intermetallics, sigma phase is the most prevalent, with only a few Mn-rich spots from the FeMn system predicted as A13-type BCC phase. This kind of prediction is accurate for the FeMn-CoNi-Cr diffusion multiple, but not for the Co-CrNi-FeMn multiple, neither for the Co30Cr-Ni-FeMn multiple. It is worth noting that the TCHEA2.1 database is more accurate for the sigma phase prediction than the TCFE10 database, which is evident for the predictions shown for the CoNi-FeMn-Cr multiple as very little intermetallic phases are predicted to form at 1000 °C in these composition ranges. For both Co-CrNi-FeMn and Co30Cr-Ni-FeMn system, the phases at the boundary between Co and FeMn and the phases at the boundary between Co30Cr and FeMn are either indexed as FCC or HCP by EBSD with no intermetallic phase detected.

At 425 °C, there is an evident lack of data to correctly predict phase stability using the TCHEA2.1 database, which do not even bring qualitative phase prediction. As for the TCFE10 database, the HCP phase appears in both the Co-CrNi-FeMn and the Co30Cr-Ni-FeMn multiples, although this result does not correspond to the experimentally observed phases neither. However, Thermo-Calc

Journal : Large 11669 Dispatch : 24-6-2021 Pages : 12
Article No. : 902 LE TYPESET
MS Code : JPED-21-03-2509 CP DISK

predicts CoFe and MnNi to be BCC, which is observed experimentally in the CoFe-MnNi-Cr multiple.

Overall, currently available tools, even at the state of the art, cannot accurately predict phase formation in diffusion multiples. However, these tools still are of interest for alloy design, proposing trends for phase stability at high temperature. To become a predictive tool, CALPHAD databases need to be improved.

It is shown that diffusion multiples can be a great method to complement CALPHAD or other computational tools. However, great care is necessary to produce valid samples as even a small number of impurities can have a large impact on phase stability due to the large reactivity of some of them. As shown in Fig. 4, a very small amount of residual carbon present in one of the Cr raw material used for the building up of multiples brings a huge change of phases and microstructure morphology in a specific range of compositions. The prolonged heat treatment carried out to activate the diffusion of substitutional elements combined with the much faster diffusion of interstitial carbon bring some kind of "cleaning" of carbon from a large part of the multiple and its concentration in a specific zone where $M_{23}C_6$ formation was activated. The formation of this carbide has also been reported by Wilson *et al.* on a similar diffusion multiple [25]. The presence of this residual carbon has also a large influence on the formation of the sigma phase.

4.2 Inter-diffusion in HEAs

The diffusion multiple approaches can be used to determine interdiffusion coefficients. However, estimation of diffusion parameters becomes exponentially more complicated with an increasing number of elements for a given system. An adapted methodology has been proposed to extract the interdiffusion coefficients for high order systems [28,29]. However, it requires careful preparation and choice of diffusion multiples. Moreover, it assumes a single phase across the whole diffusion multiple, severely constraining the systems that can be studied by such an approach.

While diffusion coefficients cannot be determined using the multiples presented in this study, trends can be observed and discussed. To represent regions with high mixing, Figure 12 proposes a configurational entropy map for each diffusion multiple computed using Boltzmann's entropy formula, $S = -R\sum x_i \ln(x_i)$. Even though the heat treatment is identical for all samples, the choice of initial alloy has a large impact on the size of high entropy regions. In particular, the CoFe-MnNi-Cr multiple presents the largest area with an entropy greater larger than 1.5*R* after 24 h at 1000 °C. This is also the only sample where this high entropy region is not constrained inside the acquired EDX map. This can be related to the CoFe-MnNi boundary that does not meet the Cr block perpendicularly, offering a zone of decreasing distance with respect to the Cr block over more than 300 µm. This reduces the diffusion length between the elements to form a region where all five elements would be present in large amount.

Another indicator of effective inter-mixing is to define an *n*-element alloy as an alloy that possesses at least 5 at.% of *n* elements. The area corresponding to a ternary, quaternary, or quinary region measured for each diffusion multiple are given in Table 2 for both heat treatment. The AQ3 same trends as with the configurational entropy is observed. At 1000 °C, the diffusion multiple with the largest area with high mixing is the CoFe-MnNi-Cr multiple. Then, in order of decreasing multiple with large diffusion lengths, FeMn-CoNi-Cr, Co-CrNi-FeMn, and Co30Cr-Ni-FeMn, respectively.

The tracer diffusion coefficient methodology of the constitutive elements of the Cantor alloy have been

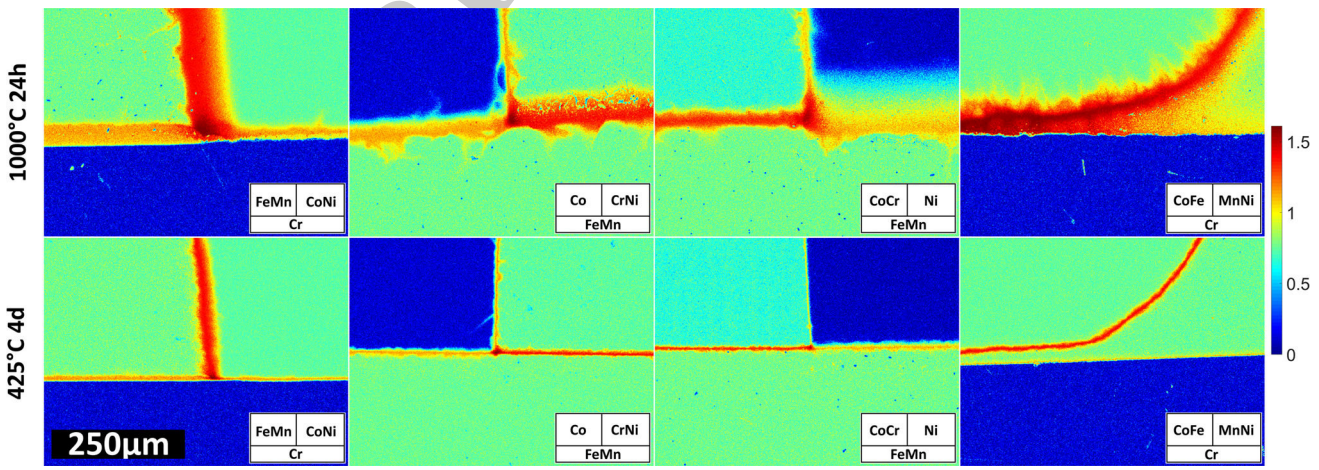

Fig. 12 Entropy map of each diffusion multiple computed using the Boltzmann's entropy formula and EDX composition maps

Journal : Large 11669 Dispatch : 24-6-2021 Pages : 12
Article No. : 902 LE TYPESET
MS Code : JPED-21-03-2509 CP DISK

Table 2 Percentages of the EDX mappings that contains more than 3, 4, or 5 elements (i.e. contains more than 5%.at of x element(s)) and percentages of the EDX mappings with Boltzmann entropy larger than ln(4) or 1.5

	5 elements, μm^2, %	4 elements, μm^2, %	3 elements, μ m^2, %	$\Delta S > 1.5R$, μm^2, %	$\Delta S > \ln(4)R$, μm^2, %
1000C24h					
FeMn-CoNi-Cr	1500 (0.8)	10875 (5.8)	19500 (10.4)	806.3 (0.43)	3375 (1.80)
Co-CrNi-FeMn	562.5 (0.3)	9000 (4.8)	20250 (10.8)	243.8 (0.13)	1668.8 (0.89)
Co30Cr-Ni-FeMn	562.5 (0.3)	6937.5 (3.7)	24187.5 (12.9)	131.3 (0.07)	862.5 (0.46)
CoFe-MnNi-Cr	11250 (6.0)	13687.5 (7.3)	18375 (9.8)	5512.5 (2.94)	11906.3 (6.35)
425C4d					
FeMn-CoNi-Cr	187.5 (0.1)	4875 (2.6)	7500 (4.0)	56.25 (0.03)	731.3 (0.39)
Co-CrNi-FeMn	187.5 (0.1)	1875 (1.0)	5625 (3.0)	37.5 (0.02)	243.8 (0.13)
Co30Cr-Ni-FeMn	0 (0)	1312.5 (0.7)	5250 (2.8)	0 (0)	75 (0.04)
CoFe-MnNi-Cr	0 (0)	4125 (2.2)	3937.5 (2.1)	0 (0)	337.5 (0.18)

reported in the literature [55–57]. In FCC alloys, at homologous temperature, the elements rank from Ni to Co to Fe to Cr to Mn from slowest to fastest diffusion species. Moreover, melting temperature will also change with the alloy constitutive elements. Considering the Cantor alloy, Mn additions will bring a decrease of its melting temperature while Cr additions bring an increase of the alloy melting temperature of the alloy. This agrees with the observed concentration gradients across the diffusion multiples where Mn consistently diffuse on a larger length than the other elements.

4.3 Mechanical Properties Prediction

Methods of local estimation of mechanical properties are scarce. Thanks to nanoindentation, Young's modulus and hardness of a tiny volume can be estimated. However, these local material properties are often hard to extrapolate to macroscopic mechanical parameters. Nevertheless, they can constitute a good indicator of interest for a specific range of compositions. Regions of interest were characterized by this method for different diffusion multiples. Representative results were presented in Fig. 7 for the triple junction of the Co-CrNi-FeMn mutliple. Hardness and yield strength are related as they depend on the same deformation mechanisms. Both mechanical properties follow the same trends [58]. However, the yield strength prediction presented here are not in agreement with the experimental indentation results.

The largest hardness is not measured in the region presenting the highest mixing, but slightly above it, in a mostly ternary region, Cr-Co-Ni. This is in agreement with experimental and calculated results of Coury *et al.* [59]. Based on state-of-the-art models for solid solution strengthening in high entropy alloys, derived by Toda-Caraballo *et al.* [60] and Varvenne *et al.* [61,62] respectively, maximum strength was attained by the alloy Cr45Co27.5Ni27.5 in the CrCoMnNi system. Moreover, Coury *et al.* evaluated the strength of Cr25Co37.5Ni37.5, Cr33.3Co33.3Ni33.3, Cr33.3Mn10Co28.3Ni28.3, and Cr45Co27.5Ni27.5 at 223,235, 243, and 258 MPa, respectively. The same alloys are evaluated at 203, 324, 212, and 815 MPa using Thermo-Calc and TCHEA2.1 database.

5 Conclusion

In summary, we showed that diffusion multiples can be a great tool to experimentally assess compositionally complex systems such as high entropy alloys, particularly in the case of the Cantor system Co-Cr-Mn-Fe-Ni. To properly explore the large composition range of such systems, it is of great importance to produce several diffusion multiples with various configurations to study the different possible diffusion paths. We have shown that this method can shed light on several aspects of alloy design such as phase prediction, inter-diffusion, and mechanical properties. Especially, it can be useful for phase prediction as the currently available computational tools are not yet accurate enough to predict stable phases, particularly at low temperatures. It is worth noting that investigating several diffusion multiples is work intensive, while great care is necessary to avoid potential contamination, which can greatly affect the outcome of the experiments.

Supplementary Information The online version contains supplementary material available at https://doi.org/10.1007/s11669-021-00902-z.

Acknowledgments The research was funded by the Walloon Region under the agreement No. 1610154-EntroTough in the context of the 2016 WallInnov call. L. Ding and H. Idrissi are acknowledged for the

Journal : Large 11669 Dispatch : 24-6-2021 Pages : 12
Article No. : 902 ☐ LE ☐ TYPESET
MS Code : JPED-21-03-2509 ☑ CP ☑ DISK

TEM analysis. This work has been performed with the help of the Lacami technological platform of UCLouvain.

References

1. M. Walbrühl, D. Linder, J. Ågren, and A. Borgenstam, Modelling of Solid Solution Strengthening in Multicomponent Alloys, *Mater. Sci. Eng. A*, 2017, **700**, p 301–311. https://doi.org/10.1016/j.msea.2017.06.001
2. O.N. Senkov, D.B. Miracle, K.J. Chaput, and J.-P. Couzinie, Development and Exploration of Refractory High Entropy Alloys—A Review, *J. Mater. Res.*, 2018, **33**(19), p 3092–3128. https://doi.org/10.1557/jmr.2018.153
3. E.J. Pickering, and N.G. Jones, High-Entropy Alloys: A Critical Assessment of Their Founding Principles and Future Prospects, *Int. Mater. Rev.*, 2016, **61**(3), p 183–202. https://doi.org/10.1080/09506608.2016.1180020
4. H. Luo, Z. Li, and D. Raabe, Hydrogen Enhances Strength and Ductility of an Equiatomic High-Entropy Alloy, *Sci. Rep.*, 2017, **7**(1), p 9892. https://doi.org/10.1038/s41598-017-10774-4
5. Y. Shi, B. Yang, and P. Liaw, Corrosion-Resistant High-Entropy Alloys: A Review, *Metals*, 2017, **7**(2), p 43. https://doi.org/10.3390/met7020043
6. V.M. Gopinath, and S. Arulvel, A Review on the Steels, Alloys/High Entropy Alloys, Composites and Coatings used in High Temperature Wear Applications, *Mater. Today Proc.*, 2020. https://doi.org/10.1016/j.matpr.2020.06.495
7. W.-Y. Chen, X. Liu, Y. Chen, J.-W. Yeh, K.-K. Tseng, and K. Natesan, Irradiation Effects in High Entropy Alloys and 316H Stainless Steel at 300 °C, *J. Nucl. Mater.*, 2018, **510**, p 421–430. https://doi.org/10.1016/j.jnucmat.2018.08.031
8. D.B. Miracle, and O.N. Senkov, A Critical Review of High Entropy Alloys and Related Concepts, *Acta Mater.*, 2017, **122**, p 448–511.
9. E.P. George, D. Raabe, and R.O. Ritchie, High-Entropy Alloys, *Nat. Rev. Mater.*, 2019, **4**(8), p 515–534.
10. B. Cantor, I. Chang, P. Knight, and A. Vincent, Microstructural Development in Equiatomic Multicomponent Alloys, *Mater. Sci. Eng. A*, 2004, **375**, p 213–218.
11. Z. Wu, H. Bei, G.M. Pharr, and E.P. George, Temperature Dependence of the Mechanical Properties of Equiatomic Solid Solution Alloys with Face-Centered Cubic Crystal Structures, *Acta Mater.*, 2014, **81**, p 428–441.
12. G. Laplanche, A. Kostka, O. Horst, G. Eggeler, and E. George, Microstructure Evolution and Critical Stress for Twinning in the CrMnFeCoNi High-Entropy Alloy, *Acta Mater.*, 2016, **118**, p 152–163.
13. H. Luo, Z. Li, A.M. Mingers, and D. Raabe, Corrosion Behavior of an Equiatomic CoCrFeMnNi High-Entropy Alloy Compared with 304 Stainless Steels in Sulfuric Acid Solution, *Corros. Sci.*, 2018, **134**, p 131–139.
14. B. Gludovatz, A. Hohenwarter, D. Catoor, E.H. Chang, E.P. George, and R.O. Ritchie, A Fracture-Resistant High-Entropy Alloy for Cryogenic Applications, *Science*, 2014, **345**(6201), p 1153–1158.
15. B. Gludovatz et al., Exceptional Damage-Tolerance of a Medium-Entropy Alloy CrCoNi at Cryogenic Temperatures, *Nat. Commun.*, 2016, **7**, p 10602.yyy
16. S. Gorsse, and O. Senkov, About the Reliability of CALPHAD Predictions in Multicomponent Systems, *Entropy*, 2018, **20**(12), p 899.
17. S. Gorsse, and F. Tancret, Current and Emerging Practices of CALPHAD Toward the Development of High Entropy Alloys and Complex Concentrated Alloys, *J. Mater. Res.*, 2018, **33**(19), p 2899–2923.
18. Z. Li, A. Ludwig, A. Savan, H. Springer, and D. Raabe, Combinatorial Metallurgical Synthesis and Processing of High-Entropy Alloys, *J. Mater. Res.*, 2018, **33**(19), p 3156–3169.
19. A. Kauffmann et al., Combinatorial Exploration of the High Entropy Alloy System Co-Cr-Fe-Mn-Ni, *Surf. Coat. Technol.*, 2017, **325**, p 174–180. https://doi.org/10.1016/j.surfcoat.2017.06.041
20. A. Akbari, and T.J. Balk, Combinatorial Thin Film Screening to Identify Single-Phase, Non-equiatomic High Entropy Alloys in the MnFeCoNiCu System, *MRS Commun.*, 2019, **9**(2), p 750–755. https://doi.org/10.1557/mrc.2019.53
21. M. Li, and K.M. Flores, Laser Processing as a High-Throughput Method to Investigate Microstructure-Processing-Property Relationships in Multiprincipal Element Alloys, *J. Alloys Compd.*, 2020, **825**, 154025. https://doi.org/10.1016/j.jallcom.2020.154025
22. J.-C. Zhao, M.R. Jackson, L.A. Peluso, and L.N. Brewer, A Diffusion Multiple Approach for the Accelerated Design of Structural Materials, *MRS Bull.*, 2002, **27**(4), p 324–329.
23. J.-C. Zhao, M.R. Jackson, and L.A. Peluso, Determination of the Nb–Cr–Si Phase Diagram Using Diffusion Multiples, *Acta Mater.*, 2003, **51**(20), p 6395–6405. https://doi.org/10.1016/j.actamat.2003.08.007
24. J.-C. Zhao, M.R. Jackson, and L.A. Peluso, Mapping of the Nb–Ti–Si Phase Diagram Using Diffusion Multiples, *Mater. Sci. Eng. A*, 2004, **372**(1–2), p 21–27. https://doi.org/10.1016/j.msea.2003.08.008
25. P. Wilson, R. Field, and M. Kaufman, The Use of Diffusion Multiples to Examine the Compositional Dependence of Phase Stability and Hardness of the Co-Cr-Fe-Mn-Ni High Entropy Alloy System, *Intermetallics*, 2016, **75**, p 15–24.
26. F.G. Coury, P. Wilson, K.D. Clarke, M.J. Kaufman, and A.J. Clarke, High-Throughput Solid Solution Strengthening Characterization in High Entropy Alloys, *Acta Mater.*, 2019, **167**, p 1–11.
27. N. Esakkiraja, and A. Paul, A Novel Concept of Pseudo Ternary Diffusion Couple for the Estimation of Diffusion Coefficients in Multicomponent Systems, *Scr. Mater.*, 2018, **147**, p 79–82. https://doi.org/10.1016/j.scriptamat.2018.01.002
28. N. Esakkiraja, K. Pandey, A. Dash, and A. Paul, Pseudo-Binary and Pseudo-Ternary Diffusion Couple Methods for Estimation of the Diffusion Coefficients in Multicomponent Systems and High Entropy Alloys, *Philos. Mag.*, 2019, **99**(18), p 2236–2264. https://doi.org/10.1080/14786435.2019.1619027
29. C.-H. Xia, S.-L. Xia, Y. Li, and X.-G. Lu, Evaluating Atomic Mobility and Interdiffusivity Based on Two-Dimensional Diffusion Simulations and Diffusion Triple Experiments, *Scr. Mater.*, 2020, **188**, p 124–129. https://doi.org/10.1016/j.scriptamat.2020.07.026
30. B.C. De Cooman, Y. Estrin, and S.K. Kim, Twinning-Induced Plasticity (TWIP) Steels, *Acta Mater.*, 2018, **142**, p 283–362. https://doi.org/10.1016/j.actamat.2017.06.046
31. Z. Li, K.G. Pradeep, Y. Deng, D. Raabe, and C.C. Tasan, Metastable High-Entropy Dual-Phase Alloys Overcome the Strength–Ductility Trade-Off, *Nature*, 2016, **534**(7606), p 227–230. https://doi.org/10.1038/nature17981
32. F. He, Z. Wang, Q. Wu, J. Li, J. Wang, and C.T. Liu, Phase Separation of Metastable CoCrFeNi High Entropy Alloy at Intermediate Temperatures, *Scr. Mater.*, 2017, **126**, p 15–19. https://doi.org/10.1016/j.scriptamat.2016.08.008
33. F. Otto et al., Decomposition of the Single-Phase High-Entropy Alloy CrMnFeCoNi After Prolonged Anneals at Intermediate Temperatures, *Acta Mater.*, 2016, **112**, p 40–52. https://doi.org/10.1016/j.actamat.2016.04.005

Journal : Large 11669 | Dispatch : 24-6-2021 | Pages : 12
Article No. : 902 | ☐ LE | ☐ TYPESET
MS Code : JPED-21-03-2509 | ☑ CP | ☑ DISK

34. E.J. Pickering, R. Muñoz-Moreno, H.J. Stone, and N.G. Jones, Precipitation in the Equiatomic High-Entropy Alloy CrMnFeCoNi, *Scr. Mater.*, 2016, **113**, p 106–109. https://doi.org/10.1016/j.scriptamat.2015.10.025
35. G. Laplanche, S. Berglund, C. Reinhart, A. Kostka, F. Fox, and E.P. George, Phase Stability and Kinetics of σ-Phase Precipitation in CrMnFeCoNi High-Entropy Alloys, *Acta Mater.*, 2018, **161**, p 338–351. https://doi.org/10.1016/j.actamat.2018.09.040
36. G. Laplanche, Growth Kinetics of σ-Phase Precipitates and Underlying Diffusion Processes in CrMnFeCoNi High-Entropy Alloys, *Acta Mater.*, 2020, **199**, p 193–208. https://doi.org/10.1016/j.actamat.2020.08.023
37. Scientific Group Thermodata Europe (SGTE), 'Binary System Cr-Ni', in *Ternary Steel Systems: Phase Diagrams and Phase Transition Data*, P. Franke and H. J. Seifert, Eds. Berlin: Springer, 2012, pp. 24–24.
38. P. Franke, D. Neuschütz, and Scientific Group Thermodata Europe (SGTE), 'Co-Cr', in *Binary systems. Part 2: Elements and Binary Systems from B – C to Cr – Zr*, vol. 19B2, P. Franke and D. Neuschütz, Eds. Berlin/Heidelberg: Springer-Verlag, 2004, pp. 1–5.
39. Scientific Group Thermodata Europe (SGTE), 'Binary System Mn-Ni', in *Ternary Steel Systems: Phase Diagrams and Phase Transition Data*, P. Franke and H. J. Seifert, Eds. Berlin, Heidelberg: Springer Berlin Heidelberg, 2012, pp. 39–39.
40. G. Laplanche, A. Kostka, C. Reinhart, J. Hunfeld, G. Eggeler, and E.P. George, Reasons for the Superior Mechanical Properties of Medium-Entropy CrCoNi Compared to High-Entropy CrMnFeCoNi, *Acta Mater.*, 2017, **128**, p 292–303. https://doi.org/10.1016/j.actamat.2017.02.036
41. J. Miao et al., The Evolution of the Deformation Substructure in a Ni-Co-Cr Equiatomic Solid Solution Alloy, *Acta Mater.*, 2017, **132**, p 35–48. https://doi.org/10.1016/j.actamat.2017.04.033
42. C.E. Slone, S. Chakraborty, J. Miao, E.P. George, M.J. Mills, and S.R. Niezgoda, Influence of Deformation Induced Nanoscale Twinning and FCC-HCP Transformation on Hardening and Texture Development in Medium-Entropy CrCoNi Alloy, *Acta Mater.*, 2018, **158**, p 38–52. https://doi.org/10.1016/j.actamat.2018.07.028
43. D. Mercier *et al.*, 'Mechanical properties mapping of cast bimetallic work roll shell material by nanoindentation', 2018, https://doi.org/10.13140/RG.2.2.35449.16482/1.
44. J.-O. Andersson, T. Helander, L. Höglund, P. Shi, and B. Sundman, Thermo-Calc & DICTRA, Computational Tools for Materials Science, *Calphad*, 2002, **26**(2), p 273–312. https://doi.org/10.1016/S0364-5916(02)00037-8
45. G. B. Bokas, W. Chen, A. Hilhorst, P. J. Jacques, S. Gorsse, and G. Hautier, Unveiling the Thermodynamic Driving Forces for High Entropy Alloys Formation Through Big Data Ab Initio Analysis, *Scr. Mater.*
46. A.D.S.E.O. Kirkendall, Zinc Diffusion in Alpha Brass, *Trans. AIME*, 1947, **171**, p 130–142.
47. A. Paul, M.J.H. van Dal, A.A. Kodentsov, and F.J.J. van Loo, The Kirkendall Effect in Multiphase Diffusion, *Acta Mater.*, 2004, **52**(3), p 623–630. https://doi.org/10.1016/j.actamat.2003.10.007
48. Scientific Group Thermodata Europe (SGTE), 'Ternary System Cr-Fe-Mn', in *Ternary Steel Systems: Phase Diagrams and Phase Transition Data*, P. Franke and H. J. Seifert, Eds. Berlin, Heidelberg: Springer Berlin Heidelberg, 2012, pp. 355–364.
49. T. Omori et al., Experimental Determination of Phase Equilibria in the Co-Cr-Ni System, *J. Phase Equilibria Diffus.*, 2014, **35**(2), p 178–185. https://doi.org/10.1007/s11669-014-0292-z
50. H. Mao, H.-L. Chen, and Q. Chen, TCHEA1: A Thermodynamic Database Not Limited for "High Entropy" Alloys, *J. Phase Equilibria Diffus.*, 2017, **38**(4), p 353–368. https://doi.org/10.1007/s11669-017-0570-7
51. F. Tancret, I. Toda-Caraballo, E. Menou, and P.E.J. Rivera Díaz-Del-Castillo, Designing High Entropy Alloys Employing Thermodynamics and Gaussian Process Statistical Analysis, *Mater. Des.*, 2017, **115**, p 486–497. https://doi.org/10.1016/j.matdes.2016.11.049
52. Y. Lederer, C. Toher, K.S. Vecchio, and S. Curtarolo, The Search for High Entropy Alloys: A High-Throughput Ab-Initio Approach, *Acta Mater.*, 2018, **159**, p 364–383. https://doi.org/10.1016/j.actamat.2018.07.042
53. S. Dixit, V. Singhal, A. Agarwal, and A.K. Prasada Rao, Multi-label Phase-Prediction in High-Entropy-Alloys Using Artificial-Neural-Network, *Mater. Lett.*, 2020, **268**, p 127606. https://doi.org/10.1016/j.matlet.2020.127606
54. S. Gorsse, D.B. Miracle, and O.N. Senkov, Mapping the World of Complex Concentrated Alloys, *Acta Mater.*, 2017, **135**, p 177–187. https://doi.org/10.1016/j.actamat.2017.06.027
55. M. Vaidya, K.G. Pradeep, B.S. Murty, G. Wilde, and S.V. Divinski, Bulk Tracer Diffusion in CoCrFeNi and CoCrFeMnNi High Entropy Alloys, *Acta Mater.*, 2018, **146**, p 211–224. https://doi.org/10.1016/j.actamat.2017.12.052
56. D. Gaertner, J. Kottke, G. Wilde, S.V. Divinski, and Y. Chumlyakov, Tracer Diffusion in Single Crystalline CoCrFeNi and CoCrFeMnNi High Entropy Alloys, *J. Mater. Res.*, 2018, **33**(19), p 3184–3191. https://doi.org/10.1557/jmr.2018.162
57. D. Gaertner et al., Concentration-Dependent Atomic Mobilities in FCC CoCrFeMnNi High-Entropy Alloys, *Acta Mater.*, 2019, **166**, p 357–370. https://doi.org/10.1016/j.actamat.2018.12.033
58. M.D. Taylor et al., Correlations Between Nanoindentation Hardness and Macroscopic Mechanical Properties in DP980 Steels, *Mater. Sci. Eng. A*, 2014, **597**, p 431–439. https://doi.org/10.1016/j.msea.2013.12.084
59. F.G. Coury, K.D. Clarke, C.S. Kiminami, M.J. Kaufman, and A.J. Clarke, High Throughput Discovery and Design of Strong Multicomponent Metallic Solid Solutions, *Sci. Rep.*, 2018, **8**(1), p 8600. https://doi.org/10.1038/s41598-018-26830-6
60. I. Toda-Caraballo, and P.E.J. Rivera-Díaz-del-Castillo, Modelling Solid Solution Hardening in High Entropy Alloys, *Acta Mater.*, 2015, **85**, p 14–23. https://doi.org/10.1016/j.actamat.2014.11.014
61. C. Varvenne, A. Luque, and W.A. Curtin, Theory of Strengthening in fcc High Entropy Alloys, *Acta Mater.*, 2016, **118**, p 164–176. https://doi.org/10.1016/j.actamat.2016.07.040
62. C. Varvenne, G.P.M. Leyson, M. Ghazisaeidi, and W.A. Curtin, Solute Strengthening in Random Alloys, *Acta Mater.*, 2017, **124**, p 660–683. https://doi.org/10.1016/j.actamat.2016.09.046

Journal : Large 11669 | Dispatch : 24-6-2021 | Pages : 12
Article No. : 902 | ☐ LE | ☐ TYPESET
MS Code : JPED-21-03-2509 | ☑ CP | ☑ DISK

Journal : **11669**
Article : **902**

Author Query Form

Please ensure you fill out your response to the queries raised below and return this form along with your corrections

Dear Author

During the process of typesetting your article, the following queries have arisen. Please check your typeset proof carefully against the queries listed below and mark the necessary changes either directly on the proof/online grid or in the 'Author's response' area provided below

Query	Details Required	Author's Response
AQ1	The Keywords were not included in the manuscript; however, this is required as per journal standard instruction. The keywords provided in the PDF was used instead. Kindly advise if action taken is correct.	
AQ2	As per the information provided by the publisher, Figs. 3, 6-11 will be black and white in print; hence, please confirm whether we can add "colour figure online".	
AQ3	Kindly check and confirm the layout of the Table 2.	
AQ4	Reference [45] is given in list but not cited in text. Please cite in text or delete from list.	
AQ5	Kindly provide the complete details for the reference [45].	